# Synthesis of comb-shaped DNA using a non-nucleosidic branching phosphoramidite


| | |
|---|---|
| Journal: | *Organic & Biomolecular Chemistry* |
| Manuscript ID | OB-ART-03-2018-000626.R1 |
| Article Type: | Paper |
| Date Submitted by the Author: | 09-May-2018 |
| Complete List of Authors: | Ellipilli, Satheesh; Emory University Department of Chemistry<br>Phillips, John; University of Utah School of Medicine<br>Heemstra, Jennifer ; Emory University Department of Chemistry, |
| | |

# Synthesis of comb-shaped DNA using a non-nucleosidic branching phosphoramidite

Satheesh Ellipilli,[a] John D. Phillips[b] and Jennifer M. Heemstra*[a]

[a]Department of Chemistry, Emory University, 1515 Dickey Drive, Atlanta, Georgia, 30322, United states E-mail: jen.heemstra@emory.edu

[b]Department of Internal Medicine, University of Utah, Salt Lake City, Utah 84112, United States

**Abstract**

Branched DNAs (bDNAs) having comb-like structures have found wide utility in molecular diagnostics and DNA nanotechnology. bDNAs can be generated either by designing and assembling linear DNA molecules into rigid non-covalent structures or by using an orthogonally protected branching unit to synthesize covalently linked structures. Despite advantages of the covalently linked structures, use of this motif has been hampered by the challenging synthesis of appropriately protected branching monomers. We report the facile synthesis of a branching monomer having orthogonal DMT and Lev protecting groups using readily available $\delta$-velarolactone and 1,3-diaminopropan-2-ol. Using this branching monomer, a comb-shaped bDNA was synthesized having three different DNA arms. The synthesis and hybridization capability of the bDNA was assessed by fluorescence microscopy using fluorescently labeled complementary and mismatched DNA probes. Convenient access to an orthogonally protected branching monomer is anticipated to accelerate applications of bDNAs in applications including diagnostics, biosensing, gene-profiling, DNA computing, multicolor imaging, and nanotechnology.

**Introduction**

Comb polymers offer unique properties and capabilities owing to the oligomers that are arrayed in parallel along their backbones. Similarly, branched DNAs (bDNAs) can be constructed in which DNA oligonucleotides are arrayed along a synthetic or oligonucleotide backbone. The capabilities of bDNAs have been harnessed for the construction of diverse and complex DNA self-assembled structures, driving promising new applications in fields including

molecular diagnostics,[1-7] biosensors,[8, 9] and DNA computing.[10-15] Two different strategies can be employed to generate branched DNAs: (1) non-covalent assembly of linear oligonucleotides to generate a double-stranded DNA backbone having overhanging single-stranded DNA tails (Fig. 1a); (2) synthesis of a backbone having covalently attached single-stranded DNA units using a branching monomer (Fig. 1b). In the latter case, branching monomers having identical protecting groups on both arms enable the synthesis of dendrimeric DNAs, but synthesis of bDNAs having comb-like structures requires a branching monomer having two different orthogonal protecting groups. The covalent approach offers the advantages of higher stability, greater control over branching angle,[16] and decreased total quantity of DNA required.[17] Despite these advantages, the covalent approach to bDNA construction has not found wide use, likely due to the lack of conveniently available branching monomers having orthogonal protecting groups. Orthogonally protected branching phosphoramidites have been synthesized based upon cytosine or adenosine scaffolds, and subsequently used for synthesis of comb-like or lariat oligonucleotide structures. These structures have been subsequently applied as signal amplifiers for the quantification of nucleic acids[17, 18] or to monitor lariat debranching enzyme activity.[19-21] However, synthesis of these nucleoside-based branching units having orthogonal protecting groups involves complex and lengthy synthetic procedures, hindering their widespread use.

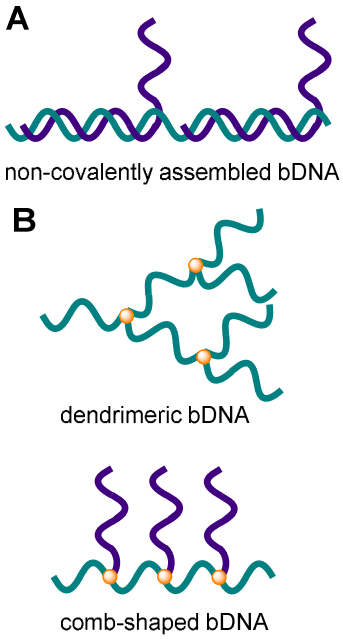


**Fig. 1**. (A) Non-covalently assembled bDNA. (B) Covalently linked dendrimeric bDNA and comb-shaped bDNA.

Here, we address this challenge through the design, synthesis, and validation of a branching phosphoramidite having dimethoxytrityl (DMT) and levuniyl (Lev) protecting groups. We have previously shown that when DMT and Lev protecting groups are present on different nucleoside phosphoramidites, these protecting groups can each be selectively removed under conditions that are compatible with DNA synthesis, enabling the construction of beads functionalized with two different oligonucleotide sequences.[22] In the current study, we utilize this protecting group strategy to synthesize an asymmetrically-protected branching phosphoramidite, which is then applied to the synthesis of a comb-like bDNA having three arms (Fig. 2). To validate bDNA synthesis, the oligonucleotides were kept attached to the solid support, and mixed with fluorescently labeled complementary or mismatched DNA sequences, then visualized using fluorescence microscopy. The beads incubated with complementary DNA probes resulted in bright fluorescence with signals at three different wavelengths, corresponding to successful hybridization to all three bDNA arms. In contrast, beads incubated with DNA probes having a single mismatch showed little to no detectable fluorescence. These results demonstrate both successful synthesis of the bDNA having three different branches and

the ability of the DNA arms to hybridize with complementary oligonucleotides when arrayed on the comb scaffold. We anticipate that this easily synthesized branching phosphoramidite will find wide use in the synthesis of bDNAs, enabling new advances in fields including biomedical diagnostics, gene-profiling, multicolor imaging, and DNA nanotechnology.

## Results and Discussion

### Synthesis of branching monomer

We hypothesized that a non-nucleosidic scaffold would provide simple access to an orthogonally-protected branching monomer, yet still be appropriate for most downstream applications. We chose DMT and Lev as the orthogonal protecting groups, as previous work from our labs had shown the ability of these groups to be individually removed under conditions that are compatible with solid-phase oligonucleotide synthesis.[22] Synthesis of branching monomer **6** was initiated by refluxing commercially available 1,3-diaminopropan-2-ol **1** with $\delta$-velarolactone to obtain **2**, having eight-atom arms to reduce steric congestion upon bDNA synthesis. Monoprotection of triol **2** with a DMT group was achieved by treatment with DMT-Cl in pyridine. We highlight that this desymmetrization step generates a racemic mixture that later gives rise to diastereomers when the branching monomer is integrated into DNA structures. However, given the flexibility of the branching monomer, we did not anticipate that this would significantly impact the overall structure and function of the comb DNAs produced, and thus we did not attempt to separate the enantiomers of **3**. Racemic DMT-protected **3** was then treated with levulinic acid under ester bond forming conditions (DIC/DMAP) to obtain orthogonally-protected levulinate esters **4** and **5**. The desired compound **4** was isolated and treated with CEP-Cl to yield racemic branching phosphoramidite monomer **6** (Scheme 1).

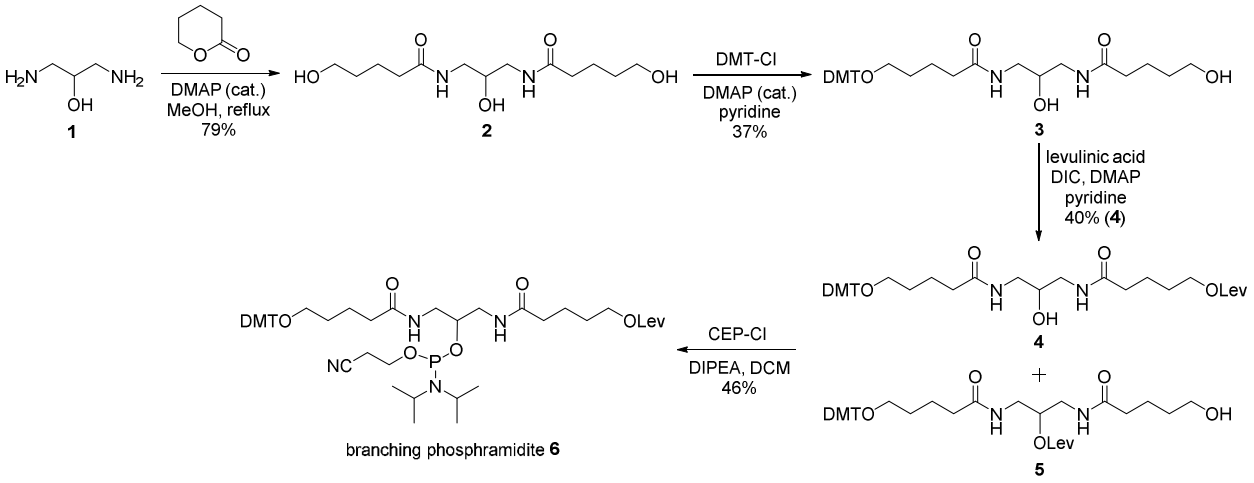


**Scheme 1**. Synthesis of branching phosphoramidite monomer.

## Design and synthesis of branched DNA

As shown in Fig. 2, beads having branched DNA were synthesized using a divergent oligonucleotide synthesis protocol. The beads were coupled with a short PEG spacer phosphoramidite, then the first branching monomer was added. Subsequent deprotection of the DMT group from the branching monomer using trichloroacetic acid (TCA), followed by sequential coupling of 12 nucleoside phosphoramidites, generated the first branch of the bDNA. To prevent further elongation, the 5′-hydroxyl of the terminal nucleoside was capped using acetic anhydride. Next, the Lev group of the branching monomer was removed using levulinyl deprotection solution (0.5 M hydrazine hydrate in 1:1 pyridine:acetic acid, Glen Research) and the hydroxyl group coupled with one PEG, followed by two thymidine phosphoramidites in order to create a spacer between the DNA arms. The second and third branches were synthesized by repeating the same steps to obtain a bDNA having three arms, each with a unique nucleotide sequence (Table 1).

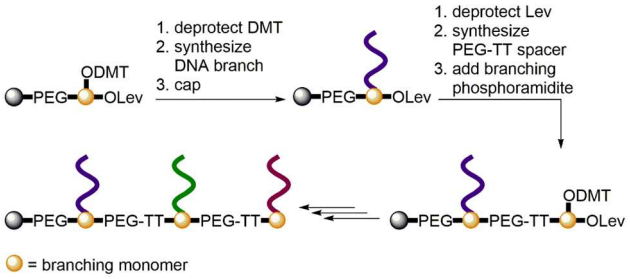


**Fig 2**. Schematic representation of branched DNA synthesis on solid support; PEG = spacer9 polyethylene glycol phosphoramidite.

**Table 1.** Sequences of bDNA arms and characterization probes. Mismatched nucleotides in smDNA probes are underlined.

| DNA | sequence (5'-3') |
|---|---|
| bDNA 1 | ATACCAGATTGT |
| bDNA 2 | GACAACGATTGC |
| bDNA 3 | ACTAACGGCTTC |
| cDNA 4 | ACAATCTGGTAT/FAM |
| cDNA 5 | GCAATCGTTGTC/ATTO550 |
| cDNA 6 | GAAGCCGTTAGT/ATTO633 |
| smDNA 7 | ACAATCTGGCAT/FAM |
| smDNA 8 | GCAATCCTTGTC/ATTO550 |
| smDNA 9 | GAACCCGTTAGT/ATTO633 |
| fmDNA 10 | CTCCGAGAACGC/FAM |
| fmDNA 11 | ATGGCTACGGTT/ATTO550 |
| fmDNA 12 | TCCATTACGCAC/ATTO633 |

Characterization of the bDNA was achieved using complementary (cDNA), single nucleotide mismatched (smDNA), and fully mismatched (fmDNA) probes for each of the DNA arms (Table 1). In the case of the smDNA probes, the mismatch site was systematically varied to explore the effect of mismatch position on selectivity of hybridization. To enable multiplexed detection, the probes for each arm were equipped with FAM, ATTO550N, or ATTO633N, which

have excitation and emission profiles that allow them to be individually imaged using fluorescence microscopy (Table 2).

**Table 2.** Excitation and emission wavelengths of probe fluorophores.

| fluorophore | excitation | emission |
|---|---|---|
| FAM 488 | 495 nm | 520 nm |
| ATTO550N | 560 nm | 575 nm |
| ATTO633N | 635 nm | 653 nm |

The bDNA-functionalized beads were incubated with all possible combinations of cDNA, smDNA or fmDNA probes (5.0 μM in 1x PBS with 0.1% tween). The samples were heated to 90 $^{O}$C for 5 min, then cooled to room temperature and the excess unhybridized DNA removed by washing with PBS. The samples were transferred into a 96-well plate and imaged using confocal microscopy. The beads incubated with all three complementary DNA probes (cDNA 4-6) showed bright fluorescence in the blue, green, and red imaging channels corresponding to the fluorophores appended to the probes (Fig. 3A). In contrast, the fluorescence images obtained for beads incubated with either single nucleotide or fully mismatched DNA probes (smDNA 7-9, & fmDNA 10-12, respectively) showed faint to no fluorescence signal (Fig. 3B & 3C, respectively). In the case of the single nucleotide mismatch probes, smDNA 7 and 8 showed faint fluorescence signals, indicating a small amount non-selective hybridization, whereas smDNA 9 showed essentially complete sequence discrimination as evidenced by no detectable fluorescence signal. As anticipated, the fully mismatched DNA probes (fmDNA 10-12) showed no fluorescence signal, indicating the lack of non-selective binding of DNA to the beads. (Fig. 3C).

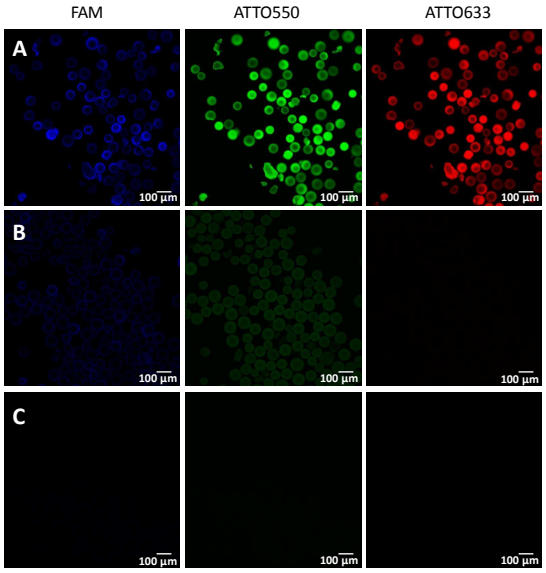


**Fig 3.** Confocal images of bDNA-functionalized beads. (A) bDNA beads incubated with complementary DNA probes cDNA 4-6; (B) bDNA beads incubated with single nucleotide mismatched DNA probes smDNA 7-9; (C) bDNA beads incubated with fully mismatched DNA probes fmDNA 10-12.

Fluorescence intensities were quantitatively assessed by analyzing images of 10-individual beads from each sample using ImageJ software. In agreement with the images shown in Figure 3, the beads incubated with all three complementary DNA probes showed high fluorescence intensities in all channels, whereas beads incubated with mismatched DNA probes showed faint to no fluorescence (Fig. 4A). To further validate the selectivity of bDNA hybridization, we imaged beads incubated with all possible combinations of two different probes within the cDNA, smDNA, and fmDNA families. As shown in Fig. 4B-D, these experiments yielded the anticipated results, with fluorescence observed in only two channels when using two complementary probes, and significantly lower to non-detectable fluorescence when using two mismatched probes. Together, these data indicate that our branching monomer enabled the synthesis of bDNA having three different sequence arms, and that each of the arms can be selectively hybridized to a complementary oligonucleotide.

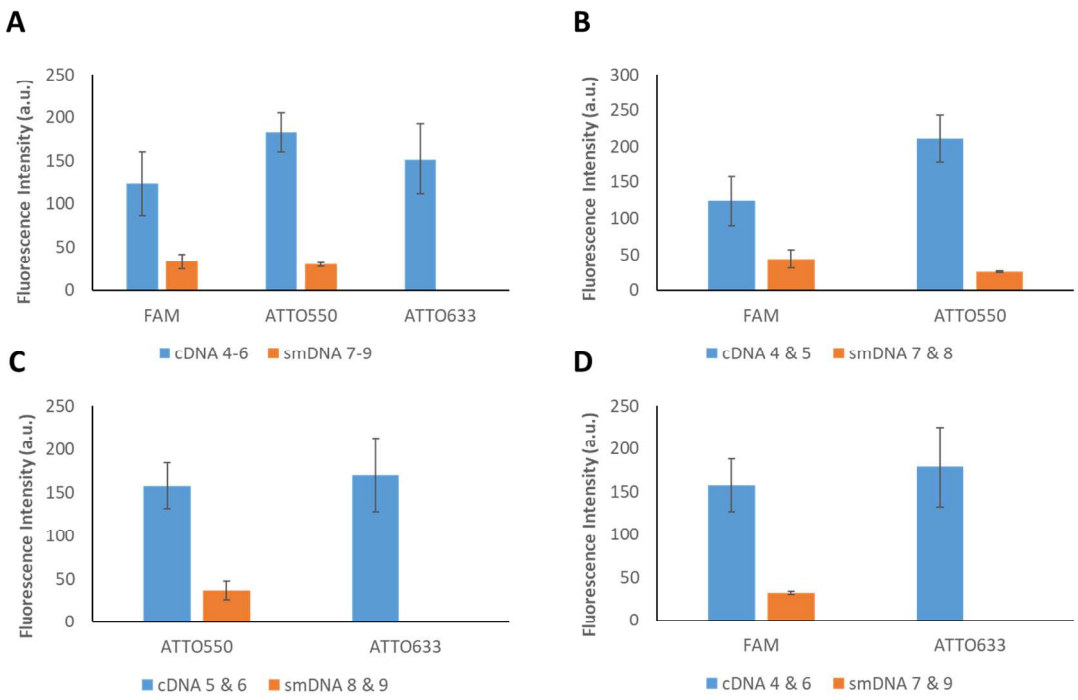


**Fig. 4** Fluorescence intensities quantified from confocal microscopy images. (A) bDNA beads incubated with cDNA 4-6 or smDNA 7-9; (B) bDNA beads incubated with cDNA 4 & 5 or smDNA 7 & 8; (C) bDNA beads incubated with cDNA 5 & 6 or smDNA 8 & 9; (D) bDNA beads incubated with cDNA 4 & 6 or smDNA 7 & 9. Fluorescence for smDNA 9 and fmDNAs 10-12 incubated with beads was not detectable.

## Conclusion

In conclusion, we present here a facile route for the synthesis of a non-nucleosidic branching phosphoramidite having orthogonal DMT and Lev protecting groups. The branching unit can be utilized in solid-phase oligonucleotide synthesis to generate a comb-shaped DNA having multiple arms with different DNA sequences. We initially synthesized a bDNA having three arms, but the oligonucleotide synthesis strategy could be easily iterated to generate comb-shaped DNAs having several more arm units appended. Characterization by fluorescence imaging revealed successful synthesis of the bDNA and selective hybridization of complementary oligonucleotide probes to each arm. While previous approaches to covalently linked bDNAs were hindered by the challenging synthesis of asymmetrically-protected branching monomers, the relative ease of our approach is anticipated to facilitate the synthesis of these biomolecular architectures. This is in turn anticipated to drive the development of new technologies in diagnostics, imaging, and nanotechnology. For example, the ability to perform

specific multivariate nucleic acid capture would enable parallel fluorescence-based analysis of multiple gene mutants relevant to human diseases or capturing of multiple unique sequences from bacteria and viruses for detection and diagnosis of infections. Using the comb as a base platform for capture or PCR amplification has distinct advantages over current technologies, including flexibility in the defined sequence spacing achievable between the "teeth" of the comb, which offers customizability to pair molecular capture to spatially-defined processes. Finally, the use of these combs as molecular bridges to juxtapose multiple stands of nucleic acids within a defined grid many be beneficial in improving the efficiency of molecular reactions such as ligation and amplification.

**Experimental Section**

**Synthesis of N,N'-(2-hydroxypropane-1,3-diyl)bis(5-hydroxypentanamide (2).** To a solution of compound **1** (3.50 g, 38.88 mmol) in methanol (25.0 mL), DMAP (0.19 g, 1.55 mmol) and $\delta$-valeroloctone (7.90 mL, 85.55 mmol) were added at room temperature. The mixture was refluxed for 12 h. After completion of the reaction, the solvent was removed *in vacuo* and the product was precipitated from 25.0 mL of dicholormethane at 4 $^{o}$C to give compound **2** as a white powder. Yield 9.0 g, 79%. $^{1}$H NMR (300 MHz, $CD_3OD$ $\delta$ 1.55-1.68 (m, 8H), 1.22-2.35 (m, 4H), 3.21-3.24 (m, 4H), 3.54-3.58 (m, 4H), 3.71 (t, 1H, *J* = 6 Hz); $^{13}$C NMR (75 MHz, $CD_3OD$) $\delta$ 16.7, 21.3, 22.2, 31.8, 31.9, 33.3, 35.6, 42.9, 61.2, 61.3, 69.1. 175.3; LRMS (ESI-TOF) *m/z* Calcd for $C_{13}H_{25}N_2O_5$ $[M + Na]^+$ 313.17; Found 313.17

**5-(bis(4-methoxyphenyl)(phenyl)methoxy)-N-(2-hydroxy-3-(5-hydroxypentanamido)propyl)pentanamide (3).** To a solution of compound **2** (4.00 g, 13.79 mmol) in pyridine (25.0 mL), DMAP (0.67 g, 5.52 mmol) and DMT-Cl (4.70 g, 13.79 mmol) were added at room temperature and the reaction mixture stirred for 12 h. After completion of the reaction, the solvent was removed *in vacuo* and the product was purified using column chromatography (10% MeOH:DCM). Yield 3.0 g, 37%. $^{1}$H NMR (300 MHz, $CDCl_3$) $\delta$ 1.53-1.71 (m, 8H), 2.15-2.25 (m, 4H), 3.04 (t, 2H, *J* = 3 Hz), 3.14-3.33 (m, 4H), 3.43 (bs, 1H), 3.58-3.60 (m, 2H), 3.69-3.71(m, 1H), 3.75 (s, 6H), 4.83 (bs, 1H), 6.78-6.81 (m, 4H), 7.27-7.39 (m, 9H); $^{13}$C NMR (75

MHz, $CDCl_3$) $\delta$ 22.1, 22.8, 29.8, 32.0, 36.1, 36.5, 42.6, 55.4, 62.1, 63.1, 86.0, 113.2, 126.9, 127.9, 128.4, 130.2, 136.7, 145.4, 158.5, 175.2. LRMS (ESI-TOF) *m/z* Calcd for $C_{34}H_{44}N_2NaO_7$ $[M + Na]^+$ 615.30; Found 615.40.

**5-((3-(5-(bis(4-methoxyphenyl)(phenyl)methoxy)pentanamido)-2-hydroxypropyl)amino)-5-oxopentyl 4-oxopentanoate (4).** To a solution of compound **3** (3.00 g, 5.07 mmol) in pyridine (25.0 mL), DMAP (620.0 mg, 5.07 mmol), DIC (1.40 mL, 10.14 mmol) and levulinic acid (880.0 mg, 7.60 mmol) were added at room temperature and the reaction mixture stirred for 12 h. After completion of the reaction, the solvent was removed *in vacuo* and the product was extracted with dichloromethane (3 x 25 mL). The organic layer was dried over anhydrous $Na_2SO_4$ and purified using column chromatography (2 % MeOH:DCM) to obtain compound **4**. Yield 1.40 g, 40%. $^1$H NMR (300 MHz, $CDCl_3$) $\delta$ 1.65-1.72 (m, 8H), 2.16-2.27 (m, 7H), 2.55 (t, 2H, *J* = 6 Hz), 2.75 (t, 2H, *J* = 6 Hz), 3.07 (t, 2H, *J* = 6 Hz), 3.21-3.38 (m, 4H), 3.72-3.75 (m, 1H), 3.79 (s, 6H), 4.10 (t, 2H, *J* = 6 Hz), 6.26 (bs, 1H), 6.49 (bs, 1H), 6.82 (d, 4H, *J* = 9 Hz), 7.19-7.32 (m, 7H), 7.42 (d, 2H, *J* = 6 Hz); $^{13}$C NMR (100 MHz, $CDCl_3$) $\delta$ 22.1, 22.6, 27.9, 29.5, 29.8, 35.8, 36.2, 37.9, 42.6, 55.1, 62.7, 63.9, 70.5, 85.7, 112.9, 126.5, 127.7, 128.1, 129.9, 136.4, 145.2, 158.2, 172.8, 174.8, 207.2; LRMS (ESI-TOF) *m/z* Calcd for $C_{39}H_{49}N_2O_9$ $[M - H]^+$ 689.34; Found 689.00.

**1-(5-(bis(4-methoxyphenyl)(phenyl)methoxy)pentanamido)-3-(5-hydroxypentanamido)propan-2-yl 4-oxopentanoate (5).** $^1$H NMR (300 MHz, $CDCl_3$) $\delta$ 1.57-1.72 (m, 8H), 2.13 (s, 3H), 2.16-2.28 (m, 4H), 2.45 (t, 2H, *J* = 6 Hz), 2.74-2.79 (m, 2H), 3.05 (t, 2H, *J* = 6 Hz), 3.24-3.34 (m, 2H), 3.43-3.55 (m, 2H), 3.58-3.63 (m, 2H), 3.76 (s, 6H),4.79-4.84 (m, 1H), 6.55 (bs, 1H), 6.80 (d, 4H, *J* = 6 Hz), 7.17-7.31 (m, 7H), 7.41 (d, 2H, *J* = 6 Hz); $^{13}$C NMR (100 MHz, $CDCl_3$) $\delta$ 21.7, 22.6, 28.1, 29.7, 31.8, 35.8, 36.3, 38.4, 38.6, 55.1, 61.9, 62.8, 71.4, 85.6, 109.9, 126.5, 127.6, 128.1, 129.9, 136.4, 145.2, 158.2, 172.0, 174.0, 208.2. LRMS (ESI-TOF) *m/z* Calcd for $C_{39}H_{49}N_2O_9$ $[M - H]^+$ 689.34; Found 689.20.

**5-((3-(5-(bis(4-methoxyphenyl)(phenyl)methoxy)pentanamido)-2-(((2-cyanoethoxy)(diisopropylamino)phosphaneyl)oxy)propyl)amino)-5-oxopentyl 4-**

**oxopentanoate (6).** To a solution of compound **4** (500.0 mg, 0.72 mmol) in dichloromethane (25.0 mL), DIPEA (0.50 mL, 2.89 mmol) and 2-cyanoethyl *N,N*-diisopropylchlorophosphoramidite (CEP-Cl, 0.16 mL, 0.79 mmol) were added at 0 $^{o}$C and stirred at room temperature for 2 h. After completion of the reaction, the mixture was diluted with dichloromethane and washed with aqueous $NaHCO_3$ solution. The organic layer was dried over anhydrous $Na_2SO_4$ and purified on neutralized silica (silica gel was stirred in trimethylamine and hexane for 1 h) and the product was eluted with 2% MeOH:DCM to obtain compound **6** as a semi-solid. Yield 300.0 mg, 46%. $^{1}$H NMR (300 MHz, $CDCl_3$) $\delta$1.12-1.21 (m, 16H), 1.66-1.70 (m, 8H), 2.18-2.25 (m, 6H), 2.55-2.74 (m, 5H), 3.05-3.07(m, 3H), 3.60-3.85 (m, 12 H), 4.06 (t, 2H, *J* = 6 Hz), 6.38-6.57 (m, 2H), 6.80 (d, 4H, *J* = 9 Hz), 7.26-7.32 (m, 8H); $^{13}$C NMR (75 MHz, $CDCl_3$) $\delta$20.5, 22.1, 23.4, 24.6, 27.9, 29.7, 35.9, 37.9, 43.2, 55.1, 58.1, 62.9, 64.1, 70.6, 85.7, 112.9, 126.5, 127.6, 128.1, 129.9, 136.5, 145.2, 158.2, 172.7, 173.6; $^{31}$P NMR (121.5 MHz, $CDCl_3$, $H_3PO_4$ as external reference) $\delta$148.18. LRMS (ESI-TOF) *m/z* Calcd for $C_{48}H_{67}N_4NaO_{10}P$ $[M + Na]^+$ 913.45; Found 913.60.

**bDNA synthesis procedure.** The bDNA was synthesized on an oligo-affinity polymeric support derivatized with 5'-dimethoxytrityl-adenosine-2',3'-diacetate using an automated DNA synthesizer (Applied Biosystems, ABI 394). The detritylation step used 6 s pulses of 3% trichloroacetic acid in $CH_2Cl_2$, followed by a 5 s wait, then the column was flushed out. This process was repeated a total of three times. The Lev deprotection was done manually using 0.5 mL of levulinyl deprotection solution for 2 x 30 s. The activator ethylthio-tetrazole was used at 0.25 M in ACN. The phosphoramidite reagents of A, T, G, C, and PEG spacer were used at 80 mM for each coupling, the doubler (D) phosphoramidite was used at 100 mM for each coupling. The coupling process consisted of three steps: 2 s addition of activator and phosphoramidite, 1 s addition of activator, and 1.5 s addition activator and phosphoramidite, followed by a 25 s wait. The capping step used a 10 s pulse of capping solution A (acetic anhydride/pyridine/THF (1:1:8 v/v)) and capping solution B (16% N-methyimidazole in THF), followed by a 5 s wait. The oxidation step used an 8 s pulse of 0.02 M Iodine in THF/pyridine/water (7:2:1 v/v), followed by a 15 s wait.

**Fluorescence bead imaging.** bDNA bead samples for confocal imaging were prepared having a concentration of 5.0 μM of each complementary or mismatched DNA probe in 1x PBS with 0.1 % tween. Each sample was heated to 90 $^{o}$C for 5 min, then slowly cooled to room temperature. The excess unhybridized DNA probe solution was removed carefully and the beads washed three times with 1x PBS. For each sample, 100 μL of 1x PBS was added and the beads were transferred to a 96-well plate. The samples were imaged on a Leica DMi8 confocal fluorescence microscope with a 10x objective using the following settings: FAM, 488 nm excitation (1.10% laser intensity, gain 50.3 v), 492-522 nm emission (band-pass); ATTO550, 561 nm excitation (67.2% laser intensity, gain 349.6 v), 567-632 nm emission (band pass); ATTO633, 633 nm excitation (35.5 % laser intensity, gain 333.7 v), 638-707 nm emission (band-pass). The confocal settings for all samples were kept constant throughout the experiment. The fluorescence intensities were acquired from confocal images by averaging the fluorescence intensities of 10 individual beads from each image using ImageJ software.

**Acknowledgements**

This work was supported by the National Institutes of Health (R01GM116991 to J.M.H. and DK110858 to J.D.P.) and the National Science Foundation (CHE 1818781 to J.M.H.).

**References**

1. C. C. Chang, C. Y. Chen, T. L. Chuang, T. H. Wu, S. C. Wei, H. Liao and C. W. Lin, *Biosens. Bioelectron.*, 2016, **78**, 200-205.
2. R. Emmadi, J. B. Boonyaratanakornkit, R. Selvarangan, V. Shyamala, B. L. Zimmer, L. Williams, B. Bryant, T. Schutzbank, M. M. Schoonmaker, J. A. Amos Wilson, L. Hall, P. Pancholi and K. Bernard, *J. Mol. Diagn.*, 2011, **13**, 583-604.
3. C. R. Ferrone, D. T. Ting, M. Shahid, I. T. Konstantinidis, F. Sabbatino, L. Goyal, T. Rice-Stitt, A. Mubeen, K. Arora, N. Bardeesey, J. Miura, T. C. Gamblin, A. X. Zhu, D. Borger, K. D. Lillemoe, M. N. Rivera and V. Deshpande, *Ann. Surg. Oncol.*, 2016, **23**, 290-296.
4. R. Firdaus, K. Saha, A. Biswas and P. C. Sadhukhan, *World J. Virol.*, 2015, **4**, 25-32.
5. Y. Li, X. Qi, C. Lei, Q. Yue and S. Zhang, *Chem. Commun.* , 2014, **50**, 9907-9909.
6. A. N. Player, L. P. Shen, D. Kenny, V. P. Antao and J. A. Kolberg, *J. Histochem. Cytochem.*, 2001, **49**, 603-612.

7. G. J. Tsongalis, *Am. J. Clin. Pathol.*, 2006, **126**, 448-453.
8. C. W. Brown, S. Buckhout-White, S. A. Díaz, J. S. Melinger, M. G. Ancona, E. R. Goldman and I. L. Medintz, *ACS Sens.*, 2017, **2**, 401-410.
9. Y. Zhao, S. Hu, H. Wang, K. Yu, Y. Guan, X. Liu, N. Li and F. Liu, *Anal. Chem.*, 2017, **89**, 6907-6914.
10. U. Feldkamp and C. M. Niemeyer, *Angew. Chem. Int. Ed. Engl.*, 2006, **45**, 1856-1876.
11. S. Kotani and W. L. Hughes, *J. Am. Chem. Soc.*, 2017, **139**, 6363-6368.
12. X. Lim, *Nature*, 2017, **546**, 687-689.
13. N. C. Seeman and H. F. Sleiman, *Nat.Rev. Mater.*, 2017, **3**, 17068.
14. F. Zhang, J. Nangreave, Y. Liu and H. Yan, *J. Am. Chem. Soc.*, 2014, **136**, 11198-11211.
15. C. LaBoda, H. Duschl and C. L. Dwyer, *Acc. Chem. Res.*, 2014, **47**, 1816-1824.
16. E. Paredes, X. Zhang, H. Ghodke, V. K. Yadavalli and S. R. Das, *ACS Nano*, 2013, **7**, 3953-3961.
17. T. Horn, C. A. Chang and M. S. Urdea, *Nucleic Acids Res*, 1997, **25**, 4842-4849.
18. T. Horn, C. A. Chang and M. S. Urdea, *Nucleic Acids Res*, 1997, **25**, 4835-4841.
19. R. S. Braich and M. J. Damha, *Bioconjugate Chemistry*, 1997, **8**, 370-377.
20. A. Katolik, R. Johnsson, E. Montemayor, J. G. Lackey, P. J. Hart and M. J. Damha, *J. Org. Chem.*, 2014, **79**, 963-975.
21. N. Tago, A. Katolik, N. E. Clark, E. J. Montemayor, K. Seio, M. Sekine, P. J. Hart and M. J. Damha, *J. Org. Chem.*, 2015, **80**, 10108-10118.
22. W. M. Hanson, Z. Chen, L. K. Jackson, M. Attaf, A. K. Sewell, J. M. Heemstra and J. D. Phillips, *J. Am. Chem. Soc.*, 2016, **138**, 11073-11076.

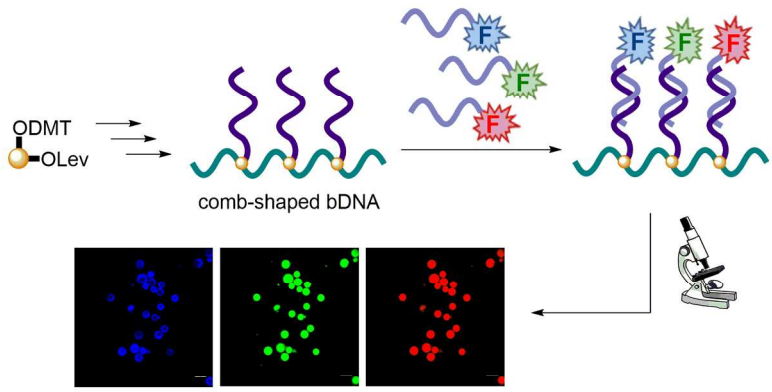


Asymmetrically-protected branching unit enables synthesis of comb-shaped DNAs for imaging and diagnostics applications.

174x81mm (300 x 300 DPI)